Journal of Geodesy (1997) 71: 320–336

Journal of Geodesy

© Springer-Verlag 1997

A canonical theory for short GPS baselines.
Part I: The baseline precision

P. J. G. Teunissen

Delft Geodetic Computing Centre (LGR), Faculty of Geodesy, Delft University of Technology, Thijsseweg 11, 2629 JA Delft, The Netherlands

Received: 16 July 1996; Accepted: 14 November 1996

Abstract. The present contribution is the first of four parts. It considers the precision of the floated and the fixed baseline. A measure is introduced for the gain in baseline precision which is experienced when the carrier phase double-differenced ambiguities are treated as integers instead of as reals. The properties of this measure are analyzed, and it is shown by means of principal angles how it relates to the change over time of the relative receiver-satellite geometry. We also present canonical forms of the baseline variance matrices for different measurement scenarios. These canonical forms make the relation between the various variance matrices transparent and thus present a simple way of studying their relative merits.

1 Introduction

As witnessed by the enormous GPS literature available, there exists a great variety in GPS models currently in use. They may range from single-site models used for local monitoring purposes to multi-baseline models used as a tool for studying geodynamic phenomena, or from supershort multi-baseline models used for local attitude determination to wide-area models for transmitting differential corrections. Depending on the application at hand, each one of these models may differ in the way the observed signals are linked, in the way the reference systems and the orbits are treated, or in the way the receiver and propagation delays are modelled. An overview of these and other GPS models, together with their applications in surveying, navigation, and geodesy, can be found in textbooks such as Borre (1995), Hofmann-Wellenhof et al. (1994), Kleusberg and Teunissen (1996), Leick (1995), Parkinson et al. (1996), or Seeber (1993).

In this contribution, which consists of four parts, we will only consider a small segment out of the rich variety of existing GPS models. The models considered are of the single-baseline type, using two stationary receivers separated by a short distance only. The term 'short' refers to the assumptions that the double-differenced GPS observables are sufficiently insensitive to orbital uncertainties in the fixed orbits and to residual ionospheric and tropospheric delays. Hence, it will be assumed that the receiver-satellite ranges and the carrier phase ambiguities are the only unknown parameters appearing in the double-differenced observation equations. Within this class of GPS models, one can discriminate between three different single-baseline models. They are:

1. the *geometry-free* model,
2. the *time-averaged* model,
3. the *geometry-based* model.

A precise definition of each of these three models will be given in the following section. It is the aim of the present contribution to give a detailed analysis of the qualities of each of these three models and to compare their relative merits. In order to provide a deeper understanding, the emphasis will be on presenting analytical results and, where possible, closed form formulae, such that a qualitative rather than a quantitative description of the intrinsic structures of both model and estimators can be given. At times however, the closed form formulae presented are also of relevance for numerical implementation.

All the analytical results are proved and summarized in theorems or corollaries. In order not to be distracted by the details of the proofs, all major proofs are collected in the Appendix. The theory to be presented is divided into four separate parts. They have been given the subtitles

I. The baseline precision,
II. The ambiguity precision and correlation,
III. The geometry of the ambiguity search space,
IV. Precision versus reliability.

Each of these four parts focusses on one major aspect of the whole process of baseline and ambiguity estimation and validation. But in all four parts, the three mentioned single-baseline models are considered. A continuous

thread that runs through the four parts is provided by the gain-number concept introduced in *Part I*. In this first part, it is the precision of both the 'floated' and the 'fixed' baseline which is analyzed. It is shown how the gain in baseline precision due to ambiguity fixing can be used to present the various baseline variance-covariance matrices in canonical form. *Part II* focusses on the ambiguities themselves; it presents an analysis of the precision and correlation of the double-differenced ambiguities as well as of the widelane ambiguities. It is shown that the first transformation of the sequence of transformations that built up the decorrelating ambiguity transformation is always given by the widelane transformation. The ambiguity search space, which is of relevance for both the estimation and the validation of the integer ambiguities, is the topic of *Part III*. A complete description of the size, shape, and orientation of the ambiguity search space is given. Finally *Part IV* considers the precision of the baseline in relation to the reliability of the ambiguities. It is shown how and to what extent an improvement in the gain in baseline precision takes place at the cost of the reliability of the ambiguities, and vice versa. Also, a measure for the ambiguity dilution of precision is introduced and closed form formulae for it are given.

The material of *Part I* is given in the present contribution. In Sect. 2 the three single-baseline models are introduced. For these models, the floated-baseline precision and the fixed-baseline precision are discussed in Sect. 3. In this section we also present an easy-to-compute second-order approximation to the baseline precision. It shows how the baseline precision depends on the observation time-span and on the sampling rate. In Sect. 4 we introduce our gain-number concept. The gain numbers measure the gain in baseline precision which is experienced when one considers the ambiguities to be integers instead of reals. It is shown how the gain numbers can be computed and how they can be interpreted as a measure for the change in relative receiver-satellite geometry. Finally in Sect. 5 we show how the gain-number concept can be used to formulate canonical forms for the various baseline variance matrices. These canonical forms make the relation between the various variance matrices transparent and thus allow one to study their relative merits. In support of this, we also present a commutative diagram of the GPS baseline precision of before and after ambiguity fixing.

2 The single-baseline model

In this section we will introduce the three single-baseline models that form the basis of our study: the *geometry-based* model, the *geometry-free* model and the *time-averaged* model. It will be assumed that double-differenced (DD) phase data are available, either on L_1 only or on both L_1 and L_2. Also, the possibility of having code data available on either L_1 or on both L_1 and L_2 is included. Furthermore it is assumed that the separation between the two GPS receivers is such that the DD observables are sufficiently insensitive to orbital uncertainties in the fixed orbits and to residual ionospheric and tropospheric delays. In order to facilitate our analysis, we will also assume that during the observation time-span, the same number m of satellites is tracked. This assumption is realistic for relatively short time-spans, as is the case when fast ambiguity fixing methods are applied.

2.1 Geometry-based model

Based on the earlier assumptions, the linear(ized) model of DD observation equations reads

$$\begin{aligned} D^T\phi_j(i) &= D^T A_i b + \lambda_j a_j \ , \\ D^T p_j(i) &= D^T A_i b \ , \end{aligned} \tag{1}$$

with $j = 1, 2$ and where $i = 1, \ldots, k$ denotes the epoch number and k equals the total number of epochs; ϕ_1, ϕ_2, p_1, and p_2 are the m-vectors containing the (observed minus computed) metric *single-differenced* (SD) phase and code observables on L_1 and L_2; D^T is the $(m-1) \times m$ DD matrix operator; A_i is the $m \times 3$ SD design matrix that captures the relative receiver-satellite geometry at epoch i; b is the 3-vector that contains the unknown increments of the three-dimensional baseline; λ_1 and λ_2 are the wavelengths of L_1 and L_2; and a_1 and a_2 are the two $(m-1)$-vectors that contain the unknown *integer* DD ambiguities; they are obtained from the SD ambiguities using the DD matrix operator already given.

The model of Eq. (1) is referred to as the geometry-based model, since the receiver-satellite geometry, as captured by the matrices A_i, plays a prominent role in it. This model forms the common mode of operation in most GPS surveying applications. Typical examples can be found in Remondi (1985), Frei and Beutler (1990), Wübbena (1991), Teunissen (1993), Tiberius and de Jonge (1995), or Goad (1996).

Note that in our description of the single-baseline model, we have explicitly shown the presence of the DD matrix operator. The reason for doing so lies in the fact that it will aid us in constructing the various canonical forms. Furthermore, the presence of the DD matrix operator will also immediately show which of the results in our analysis are reference satellite dependent and which are not.

In our analysis we assume time correlation to be absent and the time-invariant weight matrix (inverse variance matrix) at epoch i, to be given as the block diagonal matrix

$$Q^{-1} = \mathrm{diag}\,(\alpha_1, \alpha_2, \beta_1, \beta_2) \otimes \left(D^T D\right)^{-1} \ , \tag{2}$$

where '$\otimes$' denotes the Kronecker product. The scalars α_1, α_2, β_1, and β_2 are the weights of the L_1 and L_2 phase and code observables. Hence, by setting them to zero, we can short-circuit the presence of any one of these four types of observables. This will become very useful later on in the sequel, since it will allow us to use our analytical results also in situations where only a particular subset of the observables is used.

2.2 Geometry-free model

The geometry-free model follows from the geometry-based model if we disregard the presence of the receiver-satellite geometry. Hence, it follows if we replace $A_i b$ in Eq. (1) by the SD range vector r_i. The model therefore reads

$$\begin{aligned} D^T\phi_j(i) &= D^T r_i + \lambda_j a_j \ , \\ D^T p_j(i) &= D^T r_i \ , \end{aligned} \tag{3}$$

with $j = 1, 2$. Although this model is not of much use for determining the baseline, it is still a model on which one can base strategies for determining the integer ambiguities. In fact, this is the simplest approach to integer ambiguity estimation. The code data are almost directly used to determine the unknown integer ambiguities of the observed phase data. Examples of such approaches can be found in Hatch (1982), Euler and Goad (1990), Dedes and Goad (1994), Euler and Hatch (1994), and Teunissen (1996).

2.3 Time-averaged model

The time-averaged model follows from taking the time average of the vectorial observation equations of Eq. (1). It reads

$$\begin{aligned} D^T\bar{\phi}_j &= D^T\bar{A}b + \lambda_j a_j \ , \\ D^T\bar{p}_j &= D^T\bar{A}b \ , \end{aligned} \tag{4}$$

with $j = 1, 2$ and where $\bar{\phi}_j$ and $\bar{p}_j$ are the time averages of the SD phase and code data, and $\bar{A}$ is the time average of A_i.

Our motivation for including the geometry-free model and the time-averaged model in our present study is twofold. First, both these models are of practical relevance. The practical relevance of the geometry-free model has already been proven by the many applications of it. This is not yet true however for the time-averaged model. Still, it is our belief that also this model warrants a closer study in view of practical applications. The model is simpler to work with than the geometry-based model, while at the same time still relating to the baseline. Also, since the GPS receiver-satellite geometry is known to change slowly with time, the results that hold true for the time-averaged model should not differ too much from the results that hold true for the geometry-based model.

The second reason for including the geometry-free model and the time-averaged model in the present study has to do with their close relation to the geometry-based model. In fact, once we have obtained the analytical results that hold true for the geometry-based model, only minor changes have to be made in order to obtain the corresponding results that hold true for either the geometry-free model or the time-averaged model. This will therefore allow us to compare the relative merits of the three models.

One can rank the three models according to the precision of their least-squares estimators of the ambiguities. The best possible precision will be obtained with the geometry-based model and the poorest precision with the geometry-free model. The precision of the ambiguities based on the time-averaged model will generally be poorer than when using the geometry-based model, but better than when using the geometry-free model. The results of the geometry-based model become identical to those of the time-averaged model when there is no change in time of the receiver-satellite geometry. That is, when $A_i = \bar{A}$, for all i. This shows that by simply substituting $A_i = \bar{A}$, for all i in all the results that hold true for the geometry-based model, we obtain the corresponding results for the time-averaged model. It also shows that the two models are identical for the single-epoch case. In the single-epoch case, $k = 1$, the time-averaged model also becomes identical to the geometry-free model, when satellite redundancy is absent; that is when $m = 4$. Hence, this also gives us a way, free of charge, to obtain the results for the geometry-free model from those of the time-averaged model. One can also obtain the results for the geometry-free model from the results of the geometry-based model. To see this, consider the relation between the DD range vector $D^T r_i$ and the baseline b: $D^T r_i = D^T A_i b$, for $i = 1, \ldots, k$. Now simply think of vector b as an $(m-1)\,k$-vector, such that a one-to-one relation is established between b and the k $(m-1)$-vectors $D^T r_i$. In that case, the results of the geometry-based model also reduce to that of the geometry-free model.

In the present paper we will focus our attention on the geometry-based model, including its relation with the time-averaged model. The geometry-free model will not be further considered in this part, because of its parametrization in terms of the range vectors instead of the baseline. It will reappear however in *Part II*, when we start our study of the least-squares ambiguities.

3 The baseline precision

In this section we will present the variance matrices of the different least-squares estimators of the baseline vector b. Various cases will be discriminated. First, we will discriminate between the so-called '*float*' and '*fixed*' solution. The least-squares estimate of the floated baseline will be denoted as $\hat{b}$ and the least-squares estimate of the fixed baseline will be denoted as $\check{b}$. The 'float' solution follows from solving the single-baseline model in a least-squares sense, assuming that the DD ambiguities are unknown and real valued. The 'fixed' solution on the other hand, follows from solving the model in a least-squares sense, assuming that the DD ambiguities are known integers. The precision of the floated baseline will be discussed in Sect. 3.1 and the precision of the fixed baseline in Sect. 3.2.

We also discriminate between *phase-only* and *code-only* solutions. For the geometry-based model, the least-squares estimate of the floated phase-only baseline will be denoted as $\hat{b}(\phi)$ and that of the floated code-only

baseline as $\hat{b}(p)$. The least-squares estimate of the floated baseline which is based on both phase and code data will be denoted as $\hat{b}(\phi,p)$. The corresponding fixed-baseline solutions are denoted as $\check{b}(\phi)$ and $\check{b}(\phi,p)$, respectively. The estimate '$\check{b}(p)$' does not exist of course, since ambiguities are absent in the code-only case.

For the time-averaged model, no floated phase-only baseline exists. The code-only solution is denoted as $\hat{b}(\bar{p})$. The fixed-baseline solution based on phase data only is denoted as $\check{b}(\bar{\phi})$ and the fixed-baseline solution based on both phase and code data is denoted as $\check{b}(\bar{\phi},\bar{p})$.

Based on the results of the first two subsections, a second-order approximation to the baseline precision is developed in Sect. 3.3. Apart from being a viable and easy-to-compute alternative to the actual variance matrix of the baseline, our approximation also shows the main contributing factors to the baseline precision.

3.1 Before fixing

We consider the precision of the geometry-based baseline estimators $\hat{b}(\phi)$, $\hat{b}(p)$, and $\hat{b}(\phi,p)$, and the precision of the time-averaged baseline estimator $\hat{b}(\bar{p})$. It will be clear that the three types of floated baseline estimates $\hat{b}(\phi)$, $\hat{b}(p)$, and $\hat{b}(\phi,p)$ must be related, since they are based on the same model and are estimates of the same unknown baseline vector b. In fact, since $\hat{b}(\phi)$ and $\hat{b}(p)$ are uncorrelated, it follows that $\hat{b}(\phi,p)$ equals the *matrix-vector form* of the weighted average of the two. This weighted average can be written in the following two ways

$$\begin{aligned}\hat{b}(\phi,p) &= \hat{b}(\phi) + K(\phi,p)\left[\hat{b}(p) - \hat{b}(\phi)\right] \\ &= \hat{b}(p) + K(p,\phi)\left[\hat{b}(\phi) - \hat{b}(p)\right] \ .\end{aligned} \tag{5}$$

The two gain matrices $K(\phi,p) = Q_{\hat{b}}(\phi,p)Q_{\hat{b}}(p)^{-1}$ and $K(p,\phi) = Q_{\hat{b}}(\phi,p)Q_{\hat{b}}(\phi)^{-1}$ can be interpreted as *precision* gain matrices, since they measure the precision of the individual solutions $\hat{b}(p)$ and $\hat{b}(\phi)$ *relative* to the precision of the overall solution $\hat{b}(\phi,p)$. Thus if $K(\phi,p)$ is 'small', then $Q_{\hat{b}}(p)$ is 'large' with respect to $Q_{\hat{b}}(\phi,p)$ and one can expect the contribution of $\hat{b}(p)$ to be small; thus $\hat{b}(\phi,p) \simeq \hat{b}(\phi)$. Likewise, if $K(p,\phi)$ is 'small', then $Q_{\hat{b}}(\phi)$ is 'large' with respect to $Q_{\hat{b}}(\phi,p)$ and one can expect the impact of $\hat{b}(\phi)$ to be small; thus $\hat{b}(\phi,p) \simeq \hat{b}(p)$.

It will be one of our goals in this contribution to formulate, in a qualitative sense, precisely on which factors the stated gain matrices depend. In order to do so, we first need the solutions for these variance matrices. For the geometry-based model, they are given in the following theorem.

Theorem 1 (*Floated-baseline precision*)

The variance matrices of, respectively, the floated, *phase-only*, *code-only*, and *phase-and-code* baseline solutions of the geometry-based model are given as

$$\begin{aligned}Q_{\hat{b}}(\phi) &= \frac{1}{(\alpha_1+\alpha_2)}\left[\sum_{i=1}^{k}(A_i-\bar{A})^T P(A_i-\bar{A})\right]^{-1} \ , \\ Q_{\hat{b}}(p) &= \frac{1}{(\beta_1+\beta_2)}\left[\sum_{i=1}^{k}A_i^T P A_i\right]^{-1} \ , \\ Q_{\hat{b}}(\phi,p) &= \left[Q_{\hat{b}}^{-1}(p) + Q_{\hat{b}}^{-1}(\phi)\right]^{-1} \ ,\end{aligned} \tag{6}$$

with $\bar{A} = \frac{1}{k}\sum_{i=1}^{k} A_i$ and $P = D(D^TD)^{-1}D^T$.
Proof: see Appendix. □

Note that these results can also be used to determine the variance matrix of the floated baseline for the single-frequency cases. For the L_1 phase-only case, we take $Q_{\hat{b}}(\phi)$ and set $\alpha_2 = 0$. For the L_1 code-only case, we take $Q_{\hat{b}}(p)$ and set $\beta_2 = 0$ and for the phase-and-code L_1-only case, we take $Q_{\hat{b}}(\phi,p)$ and set $\alpha_2 = 0$ and $\beta_2 = 0$.

Also note that in the variance matrices three different averaging operations are involved. Namely:

- a weighted average
- a satellite average
- a time average

The weighted average manifests itself through the scale factor $1/(\alpha_1+\alpha_2)$ in $Q_{\hat{b}}(\phi)$. It is due to the weighted average that is taken in the adjustment of the L_1 and L_2 phase data: $\phi_w = (\alpha_1\phi_1 + \alpha_2\phi_2)/(\alpha_1+\alpha_2)$. The same can be said of the scale factor $1/(\beta_1+\beta_2)$ in the variance matrix of the code-only solution.

The second average involved is a satellite average. It is due to the presence of the matrix P and thus a consequence of the DD nature of the observables. The matrix P is an *orthogonal projector*, that projects orthogonally onto the range space of D. It can be represented in the following two ways

$$P = D(D^TD)^{-1}D^T = I_m - e(e^Te)^{-1}e^T \ , \tag{7}$$

with the m-vector $e = (1,\ldots,1)^T$ and the $m \times m$ unit matrix I_m. This second representation shows that with matrix P, residuals are formed with respect to the average taken over all satellites. Thus with $A_i = [a_1(t_i), \ldots a_m(t_i)]^T$ and $\bar{A} = [\bar{a}_1,\ldots,\bar{a}_m]^T$, the jth row of $P(A_i - \bar{A})$ reads as

$$(a_j(t_i) - \bar{a}_j)^T - \tfrac{1}{m}\sum_{j=1}^{m}(a_j(t_i) - \bar{a}_j)^T \ ,$$

in which the second term consists of the average over all m satellite channels. Note that this representation of the projector also makes quite clear that P is independent of the matrix representation which is chosen for D. It is thus also independent of the choice of reference satellite.

Finally, the third type of average is a time average. It manifests itself in the average over time of the individual receiver-satellite configurations, thus producing $\bar{A}$. This average is due to the presence of the time-invariant ambiguities in the phase observation equations. Note that the matrix sum of squares in the variance matrix of the phase-only solution consists of differences between the design matrices of the individual receiver-satellite

configurations and their time-averaged counterpart. This is in contrast to the variance matrix of the code-only solution, in which these differences are absent. This shows that the variance matrix of the phase-only solution depends on the *change in time* of the receiver-satellite geometry, whereas the variance matrix of the code-only solution depends on the receiver-satellite geometries at the *individual time epochs* themselves. This implies, when there would not be a change in time of the receiver-satellite geometry – thus when $k = 1$ or when $A_i = \bar{A}$, for all i – that $Q_{\hat{b}}(\phi) = \infty$, but that $Q_{\hat{b}}(p)$ would still exist.

In case of GPS, the relative receiver-satellite geometries change rather slowly due to the high-altitude orbits of the satellites. Hence, for a small observation time-span one would have $A_i \simeq \bar{A}$. This would make the matrix $\sum_{i=1}^{k}(A_i - \bar{A})^T P(A_i - \bar{A})$ near *rank defect*, thus posing potential problems in the inversion process. One should, however, not too hastily conclude from this that it implies poor estimability of the baseline. There is still the scale factor $1/(\alpha_1 + \alpha_2)$, which is very small due to the very high precision of the phase data. Hence, as to the estimability of the baseline, we see here that data precision *competes* with the change in time of the satellite geometry. But of course, one can bring the matrix $\sum_{i=1}^{k}(A_i - \bar{A})^T P(A_i - \bar{A})$ arbitrarily close to a rank-defect matrix by shortening the observation time-span. And in that case the baseline will have a poor estimability indeed.

The variance matrix of the baseline when using the time-averaged model and its relation to the baseline variance matrices of the geometry-based model can be obtained directly from Theorem 1 by assuming that the individual receiver-satellite geometries coincide with their time average. The results are summarized in the following corollary.

Corollary 1 (*Floated-baseline precision*)

The floated-baseline variance matrix of the *time-averaged* model and its relation to the floated-baseline variance matrices of the *geometry-based* model read

$$\begin{aligned} Q_{\hat{b}}(\bar{p}) &= \frac{1}{(\beta_1 + \beta_2)k}\left[\bar{A}^T P \bar{A}\right]^{-1} \quad , \\ Q_{\hat{b}}(p) &= \left[Q_{\hat{b}}(\bar{p})^{-1} + \epsilon Q_{\hat{b}}(\phi)^{-1}\right]^{-1} \quad , \\ Q_{\hat{b}}(\phi, p) &= \left[Q_{\hat{b}}(\bar{p})^{-1} + (1+\epsilon) Q_{\hat{b}}(\phi)^{-1}\right]^{-1} \quad , \end{aligned} \tag{8}$$

with the weight ratio $\epsilon = (\beta_1 + \beta_2)/(\alpha_1 + \alpha_2)$.

Proof: The first expression follows from substituting $A_i = \bar{A}$, for all i, in the expression for $Q_{\hat{b}}(p)$ of Theorem 1. The last two expressions make use of the fact that $\sum_{i=1}^{k}(A_i - \bar{A})^T P(A_i - \bar{A}) = \sum_{i=1}^{k} A_i^T P A_i - k\bar{A}^T P\bar{A}$. □

Note that a phase-only solution does not exist in case of the time-averaged model. The reason is of course due to the lack of a change in time of the receiver-satellite geometry. For the same reason, no phase-only solution exists in case of the geometry-based model, when only one epoch is taken into account.

The corollary shows that the estimators $\hat{b}(p)$ and $\hat{b}(\phi, p)$ are indeed more precise, or at the most equally precise as the estimator $\hat{b}(\bar{p})$. Equality in precision only holds when the receiver satellite fails to change in time. Still one can expect the suboptimal estimator $\hat{b}(\bar{p})$ to be close to optimal when the receiver-satellite geometry has changed only a little over time. To what extent this is true, will be made clear in the sections following.

3.2 After fixing

We will now consider the fixed-baseline solution. From the preceding discussion it will be clear that it is the presence of the unknown but time-constant ambiguities which prevents one, in case of phase data only, to determine the baseline with sufficient precision if only a short observation time-span is used. One may therefore expect a significant improvement in baseline precision if the ambiguities can be treated as known quantities. If we denote the $2(m-1)$-vector of *integer* ambiguities as $\check{a}$, the general relation between the fixed and floated least-squares estimates of the baseline can be expressed as

$$\check{b} = \hat{b} - Q_{\hat{b}\hat{a}} Q_{\hat{a}}^{-1}(\hat{a} - \check{a}) \quad . \tag{9}$$

An application of the error propagation law then gives

$$Q_{\check{b}} = Q_{\hat{b}} - Q_{\hat{b}\hat{a}} Q_{\hat{a}}^{-1} Q_{\hat{a}\hat{b}} \quad , \tag{10}$$

which shows that $Q_{\check{b}} < Q_{\hat{b}}$. Note that in the application of the error propagation law, the integer ambiguities have been treated as nonstochastic variables. Thus the given matrix is a *conditional* variance matrix. That is, it is the variance matrix of the baseline, conditioned on the assumption that the ambiguities are known and *non* stochastic. But actually, the computed ambiguities are *not* nonstochastic. The fact that the ambiguity fixing process produces an ambiguity vector which is integer, *does not* imply that it is nonstochastic. Hence, in order to obtain the theoretically correct variance matrix of $\check{b}$, the stochasticity of the integer ambiguity vector $\check{a}$ should be taken into account when applying the error propagation law to Eq. (9). This is a nontrivial problem and one that has not yet been solved satisfactorily from a theoretical point of view. Fortunately, the practical relevance of this problem diminishes when a sound procedure has been used for the validation of $\check{a}$. One of the features of a proper validation procedure should namely be to verify whether or not sufficient probability mass is located at a single grid point in the space of integers. Only when this can be assured to a sufficient degree will it be realistic to consider Eq. (10) as the variance matrix of the fixed baseline. In this, *Part I*, it will be assumed that this is indeed the case.

As in the case of the floated baseline, the phase-only and code-only solutions can be combined to give the solution based on both phase and code data. The

matrix-vector form of the weighted average can be written in the following two ways

$$\begin{aligned}\check{b}(\phi,p) &= \check{b}(\phi) + L(\phi,p)\left[\hat{b}(p) - \check{b}(\phi)\right] \\ &= \hat{b}(p) + L(p,\phi)\left[\check{b}(\phi) - \hat{b}(p)\right] \quad .\end{aligned} \tag{11}$$

Again the gain matrices $L(\phi,p) = Q_{\check{b}}(\phi,p)Q_{\hat{b}}(p)^{-1}$ and $L(p,\phi) = Q_{\check{b}}(\phi,p)Q_{\check{b}}(\phi)^{-1}$ can be seen as matrices that measure the gain experienced in baseline precision. The variance matrices on which they depend are given in the following theorem.

Theorem 2 (*Fixed-baseline precision*)

The variance matrices of the fixed *phase-only* and fixed *phase-and-code* solution of the geometry-based model, are given as

$$\begin{aligned}Q_{\check{b}}(\phi) &= \frac{1}{\alpha_1+\alpha_2}\left[\sum_{i=1}^{k} A_i^T P A_i\right]^{-1} \quad , \\ Q_{\check{b}}(\phi,p) &= \left[Q_{\hat{b}}(p)^{-1} + Q_{\check{b}}(\phi)^{-1}\right]^{-1} \quad .\end{aligned} \tag{12}$$

Proof: see Appendix. □

Comparing the results of this theorem with those of Theorem 1 shows the impact of ambiguity fixing. In particular, note that the matrix residuals $A_i - \bar{A}$ which are present in $Q_{\hat{b}}(\phi)$, are absent in $Q_{\check{b}}(\phi)$. In fact $Q_{\check{b}}(\phi)$ has become a *downscaled* version of the code-only variance matrix $Q_{\hat{b}}(p)$.

We will now consider the fixed-baseline estimator based on the time-averaged model and its relation with the corresponding estimators of the geometry-based model. As we have seen, the floated baseline of the time-averaged model was independent of the phase data. In the fixed case however, the phase data will be able to contribute to the solution of the baseline. This is due to the fact that once the ambiguities are assumed known, the phase data start to act as if they were code data. Thus $\check{b}(\bar{\phi})$ exists, whereas $\hat{b}(\bar{\phi})$ does not. Since the time-averaged phase data do not correlate with the floated phase-only solution $\hat{b}(\phi)$, again a matrix-vector form of weighted averages can be formulated. It can be represented in the following two ways:

$$\begin{aligned}\check{b}(\phi) &= \check{b}(\bar{\phi}) + G(\phi)\left[\hat{b}(\phi) - \check{b}(\bar{\phi})\right] \\ &= \hat{b}(\phi) + H(\phi)\left[\check{b}(\bar{\phi}) - \hat{b}(\phi)\right] \quad ,\end{aligned} \tag{13}$$

with the gain matrices $G(\phi) = Q_{\check{b}}(\phi)Q_{\hat{b}}(\phi)^{-1}$ and $H(\phi) = Q_{\check{b}}(\phi)Q_{\check{b}}(\bar{\phi})^{-1}$. Also $\check{b}(\bar{\phi})$ and $\hat{b}(\phi,p)$ are uncorrelated, giving the updates

$$\begin{aligned}\check{b}(\phi,p) &= \check{b}(\bar{\phi}) \quad + G(\phi,p)\left[\hat{b}(\phi,p) - \check{b}(\bar{\phi})\right] \\ &= \hat{b}(\phi,p) + H(\phi,p)\left[\check{b}(\bar{\phi}) - \hat{b}(\phi,p)\right] \quad ,\end{aligned} \tag{14}$$

with the gain matrices $G(\phi,p) = Q_{\check{b}}(\phi,p)Q_{\hat{b}}(\phi,p)^{-1}$ and $H(\phi,p) = Q_{\check{b}}(\phi,p)Q_{\check{b}}(\bar{\phi})^{-1}$. The two G matrices measure the gain that is experienced due to ambiguity fixing and the two H matrices measure the gain in precision between the suboptimal fixed baseline and its optimal counterpart. The variance matrices that determine these gains are given in the following corollary.

Corollary 2 (*Fixed-baseline precision*)

The variance matrices of the fixed *phase-only* and fixed *phase and code* solution of the time-averaged model and their relation to their counterparts of the geometry-based model, are given as

$$\begin{aligned}Q_{\check{b}}(\bar{\phi}) &= \frac{1}{(\alpha_1+\alpha_2)k}\left[\bar{A}^T P \bar{A}\right]^{-1} \quad , \\ Q_{\check{b}}(\bar{\phi},\bar{p}) &= \left[Q_{\hat{b}}(\bar{p})^{-1} + Q_{\check{b}}(\bar{\phi})^{-1}\right]^{-1} \quad , \\ Q_{\check{b}}(\phi) &= \left[Q_{\check{b}}(\bar{\phi})^{-1} + Q_{\check{b}}(\phi)^{-1}\right]^{-1} \quad , \\ Q_{\check{b}}(\phi,p) &= \left[Q_{\check{b}}(\bar{\phi})^{-1} + Q_{\hat{b}}(\phi,p)^{-1}\right]^{-1} \quad .\end{aligned} \tag{15}$$

Proof: Assuming the ambiguities to be known, the first two variance matrices follow from a least-squares adjustment of the model of Eq. (4), and the third and fourth from using the results of Theorems 1 and 2. □

If we compare the phase-only, but fixed-baseline variance matrix of the time-averaged model with the code-only, but floated-baseline variance matrix given in Corollary 1, we clearly see that after ambiguity fixing the carrier phase data start to act as if they were very precise code data. The last two equations of the corollary show how the fixed phase-only variance matrix of the time-averaged model determines the differences between the fixed- and floated-baseline variance matrices of the geometry-based model.

3.3 A second-order approximation of the baseline precision

Up to this point, we have made use of the epoch number i as a way of indexing all time-dependent variables. However, indexing with the epoch number does not make explicit the relation that exists between the epoch number and the argument of time itself. In order to make this relation explicit, we will derive in this section a second-order approximation of the precision of the baseline. It provides a way of showing how the baseline precision depends on the chosen sampling rate and the chosen observation time-span. For sufficiently short observation time-spans, our approximation may also be used as an easy to compute alternative to the actual variance matrix of the baseline. This may in particular be helpful for design computations.

Theorem 3 (*Baseline-precision to second order*)

Let the two matrices $\dot{A} = [\dot{a}_1(t_c), \ldots, \dot{a}_m(t_c)]^T$ and $\ddot{A} = [\ddot{a}_1(t_c), \ldots, \ddot{a}_m(t_c)]^T$ be the first-order and second-order time derivatives of the SD design matrix $A_i = [a_1(t_i), \ldots, a_m(t_i)]^T$, evaluated at the central time epoch $t_c = \frac{1}{k}\sum_{i=1}^{k} t_i$, with $t_i = t_0 + iT$. Then to a second order:

$$Q_{\hat{b}}(\phi, p) \doteq \frac{1}{(\alpha_1 + \alpha_2)k}\left[\epsilon\, \bar{A}^T P \bar{A} + c_1(\dot{A}^T P \dot{A} + c_2 \ddot{A}^T P \ddot{A})\right]^{-1}, \tag{16}$$

with the c-coefficients

$$c_1 = \frac{1}{12}(1 + 1/\epsilon)(1 - 1/k^2)(kT)^2 \ ,$$
$$c_2 = \frac{1}{60}(1 - (2/k)^2)(kT)^2 \ .$$

Proof: see Appendix. □

Note that the acceleration term is absent in Eq. (16) when $k = 2$, and that both the velocity and acceleration terms are absent when $k = 1$. Also note that each of the three matrices in the sum of Eq. (16) is symmetric. That is, 'cross products' like $\dot{A}^T P \ddot{A}$, are absent. This is due to the symmetric expansion around the central epoch t_c. 'Cross products' containing the acceleration term will appear however, when $\bar{A}$ is developed around t_c. But they disappear when one is willing to neglect the acceleration; and in that case the variance matrix $Q_{\hat{b}}(\phi, p)$ becomes rather straightforward to compute. It will then only depend on the receiver-satellite geometry through the two matrices $A(t_c)$ and $\dot{A}(t_c)$.

The theorem gives an approximation to the precision of the baseline *before* ambiguity fixing. The result Eq. (16) can however also be used, together with Corollary 2, to obtain the corresponding approximation to the precision of the baseline *after* ambiguity fixing. Also, the corresponding approximation to the precision of the floated baseline, based on phase data only, follows directly from the theorem. We therefore have the following corollary:

Corollary 3 (*Phase-only case*)

The variance matrix of the floated baseline, based on phase data only, reads to a second order as

$$Q_{\hat{b}}(\phi) \doteq c\left[\dot{A}^T P \dot{A} + \frac{(kT)^2}{60}(1 - (\tfrac{2}{k})^2)\ddot{A}^T P \ddot{A}\right]^{-1} \ , \tag{17}$$

with $c = 12/\left\{(kT)^2(k - \frac{1}{k})(\alpha_1 + \alpha_2)\right\}$.

Proof: simply set $\beta_1 = 0$ and $\beta_2 = 0$ in order to obtain Eq. (17) from Eq. (16). □

Based on this result, a number of remarks can be made. First note that it is indeed the *change in time* of the receiver-satellite geometry and not the instantaneous geometry itself which determines the precision of the floated phase-only baseline. Secondly, note that the time-dependent parameters in Eq. (17) appear as scale factors when the acceleration term is neglected. Hence, in this case the *structure* of the variance matrix becomes time invariant and the time-dependent part acts in the same way as a variance factor of unit weight would. This shows that the correlation between the baseline components is approximately constant, but that the level of the baseline precision is governed by the time-dependent scale factor

$$c = \frac{12}{[(k-1)T]^2(\alpha_1 + \alpha_2)}\frac{k-1}{k(k+1)} \ .$$

This also implies that the time-dependent behavior of all diagnostic quantities which are based on $Q_{\hat{b}}(\phi)$, such as the eigenvalues, the determinant or the *dilution of precision* (DOP) factors, are governed by c as well.

The corollary also makes quite clear how the baseline precision behaves as function of both the *sampling rate* and the length of the observation *time-span*. In order to study the effect of the sampling rate, one should consider a constant observation time-span. Thus in this case k varies, while $(k-1)T$ stays constant. However, in order to study the effect of the observation time-span, one should consider a constant sampling rate. Hence, in this case, $(k-1)T$ varies, while k stays constant. With this in mind, it follows from Eq. (17) that

$$Q_{\hat{b}}(\phi) \sim (k-1)/k(k+1) \quad \text{(sampling rate)} \ ,$$
$$Q_{\hat{b}}(\phi) \sim 1/[(k-1)T]^2 \quad \text{(time-span)} \ .$$

This result shows that an increase in the observation time-span is more effective in getting the variances of the baseline down to smaller values, than an increase in the sampling rate.

When code data are included as well, the situation changes. This is due to the additional term $\epsilon \bar{A}^T P \bar{A}$ in the normal matrix. The significance of this change depends on how large the phase-code variance ratio ϵ is. We return to this matter in Sect. 5.

Finally note that since the c-coefficient acts as a scale factor and since the baseline precision will be poor when the observation time-span is short, it is advisable, when inverting the actual normal matrix in order to obtain the variance matrix, to treat the above c-coefficient just as one would treat the variance factor of unit weight. If this precaution is not taken, one runs the risk, in particular with short observation time-spans, that rounding errors will destroy the inversion process.

4 The gain in baseline precision

The sole purpose of ambiguity fixing is to be able, via the inclusion of the integer constraints on the ambiguities, to improve upon the precision of the baseline. The impact of the integer constraints on the ambiguities manifests itself therefore in the change in baseline precision, when going from the 'float' situation to the 'fixed' situation. In the present section we will make a start with our study of this gain in baseline precision. In

Sect. 4.1 we will introduce our concept of gain numbers and study some of its characteristics. In Sect. 4.2, the gain numbers will be interpreted geometrically, and in Sect. 4.3, we study the time-dependent behavior of the gain numbers. Finally, in Sect. 4.4, we present a simple way of computing the gain numbers.

4.1 Gain numbers and gain vectors

In this section we introduce our concept of gain numbers and gain vectors. Gain numbers measure the gain in baseline precision due to ambiguity fixing. The corresponding gain vectors describe the direction in which the gain in baseline precision is experienced. Recall that $\hat{b}$ and $\check{b}$ are the least-squares estimates of the baseline before and after ambiguity fixing, respectively. The corresponding least-squares estimates of the baseline component $f^T b$ then read: $\hat{\theta} = f^T \hat{b}$ and $\check{\theta} = f^T \check{b}$. Since the variance ratio $\sigma^2_{\hat{\theta}} / \sigma^2_{\check{\theta}}$ measures the improvement in precision when replacing the estimate $\hat{\theta}$ by $\check{\theta}$, we introduce the following definition for the gain numbers and the gain vectors.

Definition

Gain numbers are given as the ratio

$$\gamma(f) = \frac{f^T Q_{\hat{b}}(\phi) f}{f^T Q_{\check{b}}(\phi) f} \tag{18}$$

and the corresponding vectors $f \in R^3$ are called *gain vectors*.

Note that we have defined the gain numbers for the phase-only case. It will be clear that we could have equally well defined the gain numbers for the case that phase-*and*-code data are used. In that case, the variance matrices in Eq. (18) would have to be replaced by $Q_{\hat{b}}(\phi, p)$ and $Q_{\check{b}}(\phi, p)$, respectively. The reason for using the definition given here though, is that it results in gain numbers that are *independent* of the observation weights used. Hence, the gain number $\gamma(f)$ becomes solely dependent on the receiver-satellite geometry. This will therefore allow us in our further analysis clearly to separate the impact of the observation weights from the impact of the receiver-satellite geometry.

Since the gain numbers are defined as ratios, they are dimensionless. Also note that the gain numbers are invariant to a reparametrization of the baseline. Hence, one will obtain identical gain numbers when using, for instance, a local {North, East, Up}-frame or a global geocentric frame.

The stationary values of the ratio Eq. (18) correspond with the roots of the characteristic equation $| Q_{\hat{b}}(\phi) - \gamma Q_{\check{b}}(\phi) | = 0$. In particular, let $\gamma_1 \leq \gamma_2 \leq \gamma_3$ denote the roots of this characteristic equation and let f_i, $i = 1, 2, 3$, denote the corresponding eigenvectors. Then

$$\gamma_1 = \gamma(f_1) = \min_{f \neq 0} \gamma(f) \ ,$$

$$\gamma_3 = \gamma(f_3) = \max_{f \neq 0} \gamma(f) \ .$$

This shows that the maximum improvement in precision due to ambiguity fixing equals γ_3 and is experienced in the direction f_3. Similarly, the precision improvement is minimally γ_1 and it is experienced in the direction f_1.

We also have the following *minimax* characterization for γ_2, $(f \neq 0)$:

$$\gamma_2 = \min_{a \neq 0} \max_{a^T f = 0} \gamma(f) = \max_{a \neq 0} \min_{a^T f = 0} \gamma(f) \ .$$

This shows, since

$$\max_{a^T f = 0} \gamma(f), \quad f \neq 0$$

is the maximum gain in baseline precision, that when one particular component of the baseline is fixed, γ_2 is the minimum value of all such gains for all possible one-dimensional constraints on the baseline. Hence, if for instance the height component of the baseline is fixed, then the corresponding maximum gain experienced will be larger than or equal to γ_2.

The two gain numbers γ_1 and γ_3 can also be used to put bounds on the ratio of the *position dilution of precision* (PDOP), before and after fixing. By definition we have $f^T Q_{\hat{b}}(\phi) f \leq \gamma_3 f^T Q_{\check{b}}(\phi) f$, for all f. Therefore, trace $Q_{\hat{b}}(\phi) \leq \gamma_3$ trace $Q_{\check{b}}(\phi)$. Similarly, we have for the smallest gain number the inequality trace $Q_{\hat{b}}(\phi) \geq \gamma_1$ trace $Q_{\check{b}}(\phi)$. From the two inequalities follows therefore

$$\gamma_1 \leq \frac{\text{trace } Q_{\hat{b}}(\phi)}{\text{trace } Q_{\check{b}}(\phi)} \leq \gamma_3 \ .$$

This shows that the ratio of the average baseline precision of before and after fixing will never be smaller than the smallest gain and also never larger than the largest gain.

Gain numbers cannot take on arbitrary values. The following theorem shows the range of values the gain numbers may take.

Theorem 4 (*Range of gain numbers*)

All gain numbers $\gamma(f)$ are larger than or equal to one:

(i) $\gamma(f) \geq 1$, for all $f \in R^3$;

one or more of the gain numbers γ_i, $i = 1, 2, 3$ is equal to one if the null space of matrix $\bar{A}^T P \bar{A}$ is not empty:

(ii) $\gamma_i = 1, \ i = 1, \ldots, d \ \Leftrightarrow \ \dim N(\bar{A}^T P \bar{A}) = d$;

the gain numbers γ_i, $i = 1, 2, 3$ become infinite when the receiver-satellite geometry fails to change with time:

(iii) $\gamma_i = \infty, \ i = 1, 2, 3 \ \Leftrightarrow \ A_i = \bar{A}, \ i = 1, \ldots, k$.

Proof: see Appendix. □

It will be intuitively clear that the gain numbers must be larger than or equal to one, since the whole purpose of ambiguity fixing is to improve upon the baseline precision. It may happen, however, that the ambiguity fixing fails to have an effect on the precision of *some* of the baseline components. In that case one or more of the gain numbers is equal to one. This occurs when the time-averaged DD design matrix $D^T\bar{A}$ is not of full rank. Hence, in that case there exists a configuration defect in the time-averaged receiver-satellite geometry. Also note that then $Q_{\hat{b}}(\bar{p})$ and $Q_{\check{b}}(\bar{\phi})$ will fail to exist.

4.2 Gain and principal angles

In the remaining of this, *Part I*, we will refer to the three stationary values γ_i, $i = 1, 2, 3$, of $\gamma(f)$, simply as *the* gain numbers. We have seen that these gain numbers take on values in the interval $[1, \infty)$. In some way, the actual receiver-satellite configurations over the observation time-span, must have a decisive impact in this respect. It is therefore to be expected that the gain numbers are closely linked to these receiver-satellite configurations. The following theorem, which gives a *geometric* interpretation of the gain numbers, makes this dependency precise.

Theorem 5 (*Gain numbers and principal angles*)

Let $R(U), R(V) \subset R^{mk}$ be the range spaces spanned by the columns of the two matrices

$$U = \begin{bmatrix} P(A_1 - \bar{A}) \\ \vdots \\ P(A_k - \bar{A}) \end{bmatrix} \text{ and } V = \begin{bmatrix} PA_1 \\ \vdots \\ PA_k \end{bmatrix} .$$

Then

$$\gamma_i = \frac{1}{\cos^2 \theta_i}, \quad i = 1, 2, 3, \tag{19}$$

where θ_i, $i = 1, 2, 3$, are the *principal angles* between the subspaces $R(U)$ and $R(V)$, with $0 \le \theta_1 \le \theta_2 \le \theta_3 \le \pi/2$.
Proof: see Appendix. □

Note that the matrices U and V can be interpreted as being the design matrices of *before* and *after* ambiguity fixing. Matrix U corresponds then to the design matrix before ambiguity fixing, but after the ambiguity parameters have been eliminated and matrix V to the corresponding design matrix after ambiguity fixing. The theorem shows, therefore, that the gain numbers are a direct measure for the amount of *obliquity* between the range spaces of the two design matrices U and V.

The geometric interpretation of the gain numbers can be completed by introducing the orthogonal complement of the range space of U within the space spanned by the columns of U and V. Let $P_U^{\perp}$ be the orthogonal projector that projects onto the orthogonal complement of the range space of U. Then the range space of $P_U^{\perp}V$ is the required orthogonal complement. From

$$W = P_U^{\perp}V \text{ with } W = [(P\bar{A})^T, \ldots, (P\bar{A})^T]^T$$

it follows that this orthogonal complement is given by the range space of matrix W. Note that this matrix may be interpreted as being the design matrix of our *suboptimal* baseline estimators $\hat{b}(\bar{p})$ and $\check{b}(\bar{\phi})$; those which are based on the time-averaged model.

In Fig. 1, the relation between the three range spaces of U, V, and W is shown. It follows from this geometry that if the principal angles θ_i are close to zero, the gain numbers are close to their minimum value of one and $R(V)$ is close to being orthogonal to $R(W)$.

On the other hand, if the principal angles are large, then the experienced gain in baseline precision is large and $R(V)$ is close to being coincident with $R(W)$, in which case there is almost no difference between the geometry-based model and the time-averaged model. In the intermediate case, when the principal angles are close to $\pi/4$, then the gain numbers are close to 2 and the two variance matrices $Q_{\hat{b}}(\phi)$ and $Q_{\check{b}}(\bar{\phi})$ are almost identical.

4.3 Gain and time

In the previous subsection we have seen, from a geometric point of view, that the gain numbers measure how much the individual receiver-satellite geometries differ from their mean. In this subsection we will continue this analysis, but now we will also include the argument of time.

As a preliminary step, we will first consider the scalar case and consider the 'angle' $\frac{1}{2}\pi - \theta$ between two arbitrary but smooth functions $v(t)$ and $w(t)$. The square of the cosine of this angle, for a time-interval $2T$ with midpoint t_c, is given as

$$\cos^2\left(\frac{1}{2}\pi - \theta\right) = \frac{\left[\int_{t_c-T}^{t_c+T} v(t)w(t)dt\right]^2}{\int_{t_c-T}^{t_c+T} v(t)^2 dt \int_{t_c-T}^{t_c+T} w(t)^2 dt} .$$

This definition is motivated by the fact that the complements of the principal angles, $\frac{1}{2}\pi - \theta_i$, are the angles between the two subspaces V and W. Thus if we take $w(t) = 1$, we are measuring how much the function $v(t)$ differs from a constant. Assuming $w(t)$ to be constant gives

$$\sin^2(\theta) = \frac{\left[\frac{1}{2T}\int_{t_c-T}^{t_c+T} v(t)dt\right]^2}{\left[\frac{1}{2T}\int_{t_c-T}^{t_c+T} v(t)^2 dt\right]} .$$

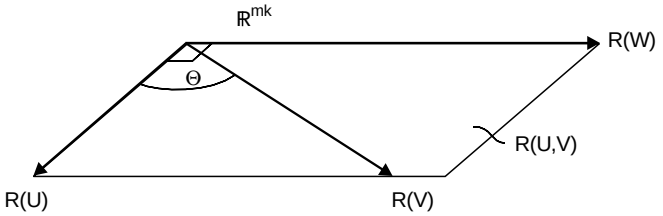

Fig. 1. The principal angles θ_i and the range spaces of U, V, and W

This is the square of a mean, divided by the mean of a square. In order to obtain the local behavior of the angle as function of the integration interval T, we develop the function $v(t)$ in its Taylor series around the midpoint t_c and perform the integration. As a result we get for $\tan^2(\theta)$, the compact expression

$$\tan^2(\theta) = 12\left(\frac{v(t_c)}{\dot{v}(t_c)}\right)^2 \frac{1}{T^2}(1 + O(T^2)) \ . \tag{20}$$

The angle between two constant functions is of course zero. Thus $\theta = \frac{1}{2}\pi$ and $\tan(\theta) = \infty$ when $\dot{v}(t_c) = 0$. The angle also goes to zero when $v(t)$ is not constant, but when the integration interval T goes to zero. Thus, the smaller the integration interval becomes, the less θ will differ from $\frac{1}{2}\pi$. And Eq. (20) clearly shows at what rate this happens. Based on this result we can expect that also the gain numbers themselves will get larger for smaller observation time-spans, with a rate that is proportional to the inverse-square of the time-span. This is made precise in the following theorem.

Theorem 6 (*Gain, sampling rate, and time-span*)

Let μ_i, $i = 1, 2, 3$, be the eigenvalues in ascending order of $| \bar{A}^T P \bar{A} - \mu \dot{A}^T P \dot{A} | = 0$. Then to a first-order approximation

$$\gamma_i - 1 = \frac{12\mu_i}{T^2(k^2 - 1)}, \quad i = 1, 2, 3, \tag{21}$$

from which it follows that

$$\begin{cases} \gamma_i - 1 = \tan^2(\theta_i) \sim \dfrac{k-1}{k+1} \text{ (sampling rate)} \\ \\ \gamma_i - 1 = \tan^2(\theta_i) \sim 1/[(k-1)T]^2 \text{ (time-span)} \ . \end{cases}$$

Proof: see Appendix. □

It is very useful to know the time dependency of the gain numbers, since many of our results, both in this contribution as in the three parts following, will be expressed in them. The theorem shows that since the gain numbers will be much larger than one for short time-spans, they themselves approximately follow an inverse-square law in the observation time-span.

Figure 2 shows a typical example of the three gain numbers γ_i, $i = 1, 2, 3$, as function of the *sampling rate* and as function of the *observation time-span*. For a fixed time-span of 300 s, Fig. 2 (top) shows the square roots of the three gain numbers as function of k. Note that the gain numbers get larger when the sampling rate increases and that we have an excellent agreement with the $\frac{k-1}{k+1}$-law of the previous theorem. It shows that the maximum factor by which the gain numbers can be enlarged through an increase in the sampling rate equals 3.

Figure 2 (bottom) shows the square roots of the three gain numbers as function of the observation time-span $(k-1)T$ for a fixed number of observation epochs of $k = 2$. Again we have an excellent agreement with the first-order approximation of the previous-theorem. Also note that the gain numbers remain significantly larger than one for a rather broad range of time-spans. This implies that within this range one will always benefit from fixing the carrier phase ambiguities.

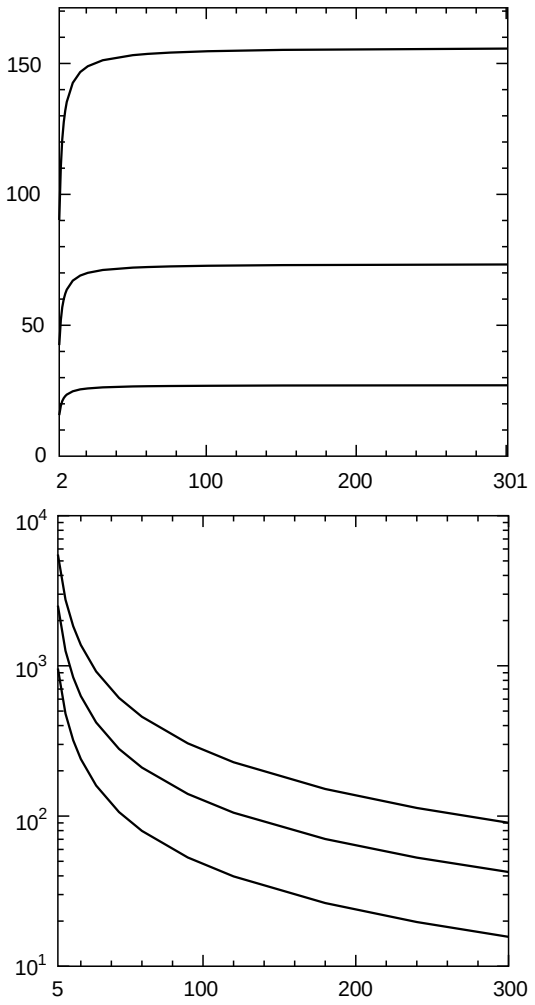

Fig. 2. The square-root gain numbers as function of k for $(k-1)T = 300$ s (*top*); The square-root gain numbers as function of $(k-1)T$ for $k = 2$ (*bottom*)

4.4 On the computation of the gain

For the numerical evaluation of γ_i, $i = 1, 2, 3$, one may use any one of the existing general-purpose algorithms for solving generalized symmetric eigenvalue problems. See, e.g., Golub and van Loan, (1989). However, since the variance matrices of the baseline are only of order 3, a more direct method of solution is also possible. This method is worked out in this subsection.

The gain numbers are given by the roots of the characteristic equation $\left|Q_{\hat{b}}(\phi) - \gamma Q_{\dot{b}}(\phi)\right| = 0$. Since $Q_{\dot{b}}(\phi)$ is positive definite, this is equivalent to

$$| Q_{\hat{b}}(\phi)Q_{\check{b}}^{-1}(\phi) - \gamma I_3 | = 0 \ .$$

Using the *Laplace expansion* for determinants, the characteristic polynomial is obtained as

$$\gamma^3 - c_1\gamma^2 + c_2\gamma - c_3 = 0 \ , \tag{22}$$

with the coefficients

$$\begin{cases} c_1 = \text{trace}\left(Q_{\hat{b}}(\phi)Q_{\check{b}}^{-1}(\phi)\right) \ , \\ c_2 = \sum_{i=1}^{3}\left(Q_{\hat{b}}(\phi)Q_{\check{b}}^{-1}(\phi)\right)_{ii} \ , \\ c_3 = \left|Q_{\hat{b}}(\phi)Q_{\check{b}}^{-1}(\phi)\right| \ , \end{cases} \tag{23}$$

where $(Q_{\hat{b}}(\phi)Q_{\check{b}}^{-1}(\phi))_{ii}$ is the cofactor of the ith-diagonal element of $Q_{\hat{b}}(\phi)Q_{\check{b}}^{-1}(\phi)$; thus, it is the determinant of the matrix of order two formed by deleting row i and column i of $(Q_{\hat{b}}(\phi)Q_{\check{b}}^{-1}(\phi))$. The roots of the cubic Eq. (22) can now be obtained as follows. Let

$$p = \tfrac{1}{3}c_2 - \tfrac{1}{9}c_1^2, \ q = \tfrac{1}{54}(2c_1^3 - 9c_1c_2 + 27c_3) \tag{24}$$

and let

$$z_1 = (q + \sqrt{r})^{1/3} \ , \quad z_2 = (q - \sqrt{r})^{1/3} \ , \tag{25}$$

with

$$r = p^3 + q^2 \ .$$

Then the three roots of Eq. (22) are given as

$$\begin{cases} \gamma_1 = z_1 + z_2 + \dfrac{1}{3}c_1 \ , \\ \gamma_2 = -\tfrac{1}{2}(z_1 + z_2) + \tfrac{1}{2}i\sqrt{3}(z_1 - z_2) + \tfrac{1}{3}c_1 \ , \\ \gamma_3 = -\tfrac{1}{2}(z_1 + z_2) - \tfrac{1}{2}i\sqrt{3}(z_1 - z_2) + \tfrac{1}{3}c_1 \ . \end{cases} \tag{26}$$

If the 'discriminant' r is positive, there will be one real root and a pair of complex conjugate roots. If $r = 0$, there will be three real roots, of which two at least are equal, and if r is negative, there will be three real unequal roots. In our case, we have $r \leq 0$. A further simplification of Eq. (26) is then possible. Writing z_1 and z_2 of Eq. (25) as $z_1 = (q + i\sqrt{-r})^{1/3}$ and $z_2 = (q - i\sqrt{-r})^{1/3}$, it follows using *Euler's relation* and $r = p^3 + q^2$ that

$$z_1 = (-p)^{1/2}\exp^{i\omega/3} \ , \quad z_2 = (-p)^{1/2}\exp^{-i\omega/3} \ , \tag{27}$$

with

$$\cos\omega = q/(-p)^{3/2} \ . \tag{28}$$

Substitution of Eq. (27) into Eq. (26) then gives

$$\begin{cases} \gamma_1 = 2(-p)^{1/2}\cos[\omega/3] + \tfrac{1}{3}c_1 \ , \\ \gamma_2 = 2(-p)^{1/2}\cos[(\omega + 2\pi)/3] + \tfrac{1}{3}c_1 \ , \\ \gamma_3 = 2(-p)^{1/2}\cos[(\omega + 4\pi)/3] + \tfrac{1}{3}c_1 \ . \end{cases} \tag{29}$$

The steps for computing the gain numbers are therefore as follows. First compute the c-coefficients according to Eq. (23). These computations are rather straightforward, since the variance matrices are only of order three. Then obtain the angle ω using Eqs. (24) and (28). The gain numbers γ_i, $i = 1, 2, 3$, then follow from substituting the angle ω, the coefficient c_1 and the variable p into Eq. (29). As a final check on the computations one may use the following root-coefficient relations of the polynomial Eq. (22)

$$\begin{cases} c_1 = \gamma_1 + \gamma_2 + \gamma_3 \ , \\ c_2 = \gamma_1\gamma_2 + \gamma_1\gamma_3 + \gamma_2\gamma_3 \ , \\ c_3 = \gamma_1\gamma_2\gamma_3 \ . \end{cases} \tag{30}$$

Once the gain numbers are obtained, the corresponding gain vectors f_i follow from solving the homogeneous equations $(Q_{\hat{b}}(\phi) - \gamma_i Q_{\check{b}}(\phi))f_i = 0$, $i = 1, 2, 3$.

5 The canonical decomposition of the baseline precision

In this section we will use the results of the previous section to develop canonical decompositions for the variance matrices of the baseline before and after ambiguity fixing. This will be done for the geometry-based model as well as the time-averaged model. In total we have eight baseline variance matrices to consider. They are the two *code-only* variance matrices $Q_{\hat{b}}(p)$ and $Q_{\hat{b}}(\bar{p})$, the three *phase-only* variance matrices $Q_{\hat{b}}(\phi)$, $Q_{\check{b}}(\phi)$ and $Q_{\check{b}}(\bar{\phi})$, and the three *phase-and-code* variance matrices $Q_{\hat{b}}(\phi,p)$, $Q_{\check{b}}(\phi,p)$, and $Q_{\check{b}}(\bar{\phi},\bar{p})$. The two variance matrices $Q_{\hat{b}}(\bar{p})$ and $Q_{\check{b}}(\bar{\phi},\bar{p})$ are of course identical, since with the time-averaged model the phase data do not contribute to the floated-baseline solution. These two matrices are therefore not treated separately.

The following theorem gives the canonical decompositions of each of these eight variance matrices. It is also at this point that we can take advantage of the fact that we have defined the gain numbers to be dependent on only the receiver-satellite geometry and thus independent of the observation weights used.

Theorem 7 (*Canonical decomposition*)

Let the gain numbers and gain vectors be collected in the two 3×3 matrices Γ and F as

$$\Gamma = \text{diag}(\gamma_1, \gamma_2, \gamma_3) \ \text{ and } \ F = (f_1, f_2, f_3) \ .$$

Then F may be normalized such that for the *code-only* case

$$\text{(i)} \ \ Q_{\hat{b}}(p) = \left[(\epsilon)FF^T\right]^{-1} \ ,$$

$$\text{(ii)} \ \ Q_{\hat{b}}(\bar{p}) = \left[\epsilon F(I_3 - \Gamma^{-1})F^T\right]^{-1} \ ,$$

and for the *phase-only* case

$$\text{(iii)} \ Q_{\check{b}}(\phi) = \left[FF^T\right]^{-1} \ ,$$

$$\text{(iv)} \ Q_{\check{b}}(\phi) = \left[F\Gamma^{-1}F^T\right]^{-1} \ ,$$

$$\text{(v)} \ Q_{\check{b}}(\bar{\phi}) = \left[F(I - \Gamma^{-1})F^T\right]^{-1} \ ,$$

and for the *phase-and-code* case

(vi) $Q_{\hat{b}}(\phi,p) = \left[(1+\epsilon)FF^T\right]^{-1}$,

(vii) $Q_{\hat{b}}(\phi,p) = \left[F(\epsilon\, I_3 + \Gamma^{-1})F^T\right]^{-1}$,

(viii) $Q_{\hat{b}}(\bar{\phi},\bar{p}) = \left[(1+\epsilon)F(I_3 - \Gamma^{-1})F^T\right]^{-1}$,

with the condition that $N(\bar{A}^T P \bar{A}) = \{\emptyset\}$ holds for the second, fifth, and eighth equality.
Proof: see the Appendix. □

The importance of the given matrix decompositions is that they *simultaneously* diagonalize the eight variance matrices with respect to the same frame F. Hence, all eight variance matrices follow once F and Γ are known. Also, the relation among these variance matrices is now directly clear, thus allowing one to study the respective gain matrices.

In order to facilitate our discussion of the results of this theorem, the variance matrices and their interrelations are shown in the commutative diagram of Fig. 3. The variance matrices are ordered columnwise as to their use of the receiver-satellite geometry and rowwise as to their dependency on the observed data. The first column of the diagram shows the variance matrices that depend only on the mean of the receiver-satellite geometry $\bar{A}$. Hence, they are the ones that follow from the time-averaged model. The second column shows the variance matrices that depend on the individual receiver-satellite geometries A_i and not explicitly on $\bar{A}$. Finally, the third column shows the variance matrices that depend both on A_i and $\bar{A}$. Rowwise, we have, from bottom to top, the variance matrices that are based on code-only data, phase-only data, and phase-and-code data, respectively.

All the arrows shown in the diagram point in the direction in which the precision of the baseline improves, assuming of course that the code data are less precise than the phase data and thus that the weight ratio is less than one, $\epsilon < 1$. Thus the variance matrix $Q_{\hat{b}}(\bar{p})$ corresponds with the poorest baseline precision and the variance matrix $Q_{\hat{b}}(\phi,p)$ with the best possible baseline precision.

The matrices shown along the arrows are the matrices with which the variance matrix at the foot of the arrow has to be premultiplied in order to obtain the variance matrix to which the arrow points. Since all arrows point in the direction in which the precision improves, all eigenvalues of the matrices along the arrows are smaller than, or at the most equal to one. These eigenvalues can be obtained directly from the matrices shown.

In order to discuss the results, we will first compare baseline estimators of which it is known a priori that one of the two always has a better precision than the other. Since the precision of the code data is much poorer than that of the phase data, we observe a tremendous improvement in baseline precision when going from the code-only solution to the *fixed* phase-only solution. This is of course also what ambiguity fixing is all about. The gain in precision for the time-averaged model is identical to the gain in precision for the geometry-based model. The gains are also identical for these two models when one goes from the fixed phase-only case to the fixed

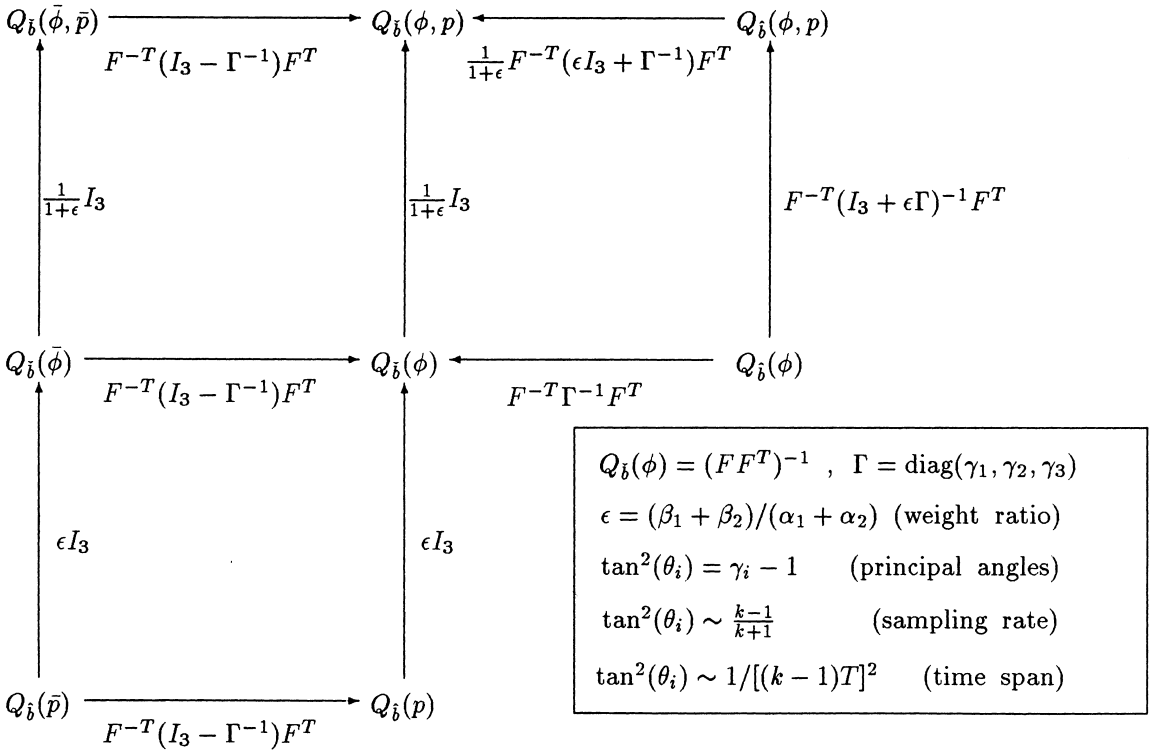

Fig. 3. Commutative diagram of GPS baseline precision, before and after ambiguity fixing

phase-and-code case. In this case however the gain is close to one, since ϵ is close to zero. This shows that once one computes a fixed baseline, the contribution of the code data is very marginal, precision wise.

When we compare the variance matrices of the time-averaged model with their counterparts of the geometry-based model, we observe that the precision of the geometry-based baseline is better by a factor that is the same for all three levels. This gain is independent of the observation weights and thus solely driven by the receiver-satellite geometry. It shows that although the time-averaged based results are suboptimal, they are very close to optimal when the gain numbers γ_i are large.

In the case of the geometry-based model, we have already noted that the inclusion of code data when computing the fixed baseline does not improve the precision of the baseline by much. When computing the floated baseline however, we have a quite different situation. In this case the precision improvement not only depends on the observation weights, but also on the receiver-satellite geometry. It depends on how large the product $\epsilon\gamma_i$ is. Thus here we see data precision competing with the receiver-satellite geometry. The precision improvement is marginal when the $\epsilon\gamma_i$ are small. Thus when computing the floated baseline, the inclusion of code data for improving the baseline precision only makes sense when the gain numbers are sufficiently large. In fact, since ϵ is very small, the float solution stops having advantage from the code data for still reasonably large values of the gain numbers. This situation will of course change when the code data become more precise. That is, the larger ϵ gets, the smaller the gain numbers need to be in order for the impact of the code data to remain marginal.

For the geometry-based model, there are two cases for which we can compare the float solution with the fixed solution; they are the phase-only solutions and the phase-and-code solutions. In the phase-only case only the receiver-satellite geometry counts, whereas in the phase-and-code case both the receiver-satellite geometry and the weight ratio count. In both cases the gain in precision is absent when the gain numbers are equal to one. And since ϵ is small, the gain will also be large in both cases when the gain numbers are large. For sufficiently large gain numbers the gain of the phase-and-code case can be approximated by $1 + 1/\epsilon$. Note that the gain of the phase-and-code case is smaller than the gain of the phase-only case. The difference between these two gains will get smaller however, the smaller the weight ratio ϵ becomes and/or the smaller the gain numbers get.

Some of the results of the preceding discussion may also be looked at in combination. For instance, since $\epsilon < 1$, $\epsilon\gamma_i \to \infty$ implies that $\gamma_i \to \infty$. It therefore follows from the diagram that if phase data fails to contribute significantly to the float solution of the geometry-based model, one might as well consider the suboptimal code-only baseline $\check{b}(\bar{p})$ instead of its optimal counterpart $\hat{b}(p)$.

So far we discussed pairs of estimators for which it is known a priori that one of the two always has a better precision. The diagram can also be used however, to identify pairs of baseline estimators for which this is not the case. Which of the two estimators has a better precision depends then on the actual receiver-satellite geometry itself or on its relation with the observation weights. We will discuss some of these pairs. First we will compare the optimal code-only solution with the optimal phase-only float solution and with the suboptimal, but fixed phase-only solution. Then we will compare the optimal fixed phase-only solution with the optimal phase-and-code float solution and with the suboptimal, but fixed phase-and-code solution.

The baseline $\hat{b}(\phi)$ is only better than $\hat{b}(p)$ when $\gamma_i < 1/\epsilon$. Thus in order for the floated phase-only solution to be better than the code-only solution, we need a not-too-short observation time-span; and this time-span needs to be longer the more precise the code data become. The baseline $\check{b}(\bar{\phi})$ is only better than $\hat{b}(p)$ when $\gamma_i > 1/(1-\epsilon)$. Since ϵ is small, this will always be the case in practice for not-too-long observation time-spans. If we combine the results of these two pairs, it follows that $\check{b}(\bar{\phi})$ is only better than $\hat{b}(\phi)$ when $\gamma_i > 2$. In this case it is only the receiver-satellite geometry that counts. Note that the principal angles are equal to $\frac{1}{4}\pi$ when $\gamma_i = 2$. In that case the relation between the three range spaces of U, V, and W of the previous section is such that the subspace $R(V)$ is 'halfway' in between $R(U)$ and $R(W)$. This is thus the 'turning point' in the receiver-satellite geometry, where the suboptimal but fixed baseline $\check{b}(\bar{\phi})$ becomes better than the optimal, but floated baseline $\hat{b}(\phi)$. In practice this will usually be the case, since one would need a rather long observation time-span to get the gain numbers down to such a small value.

Finally we compare the optimal fixed phase-only solution with the optimal phase-and-code, float solution and with the suboptimal, but fixed phase-and-code solution. The baseline $\hat{b}(\phi, p)$ is better than $\check{b}(\phi)$ when $\gamma_i < 1/(1-\epsilon)$. In practice however, this will not happen, since with the present precision of the code data it would require a very long observation time-span. The baseline $\check{b}(\phi,\bar{p})$ is better than $\check{b}(\phi)$ when $\gamma_i < 1 + 1/\epsilon$. This shows that the suboptimal phase and code solution can even be better than the optimal phase-only solution when the gain numbers are not too large. But since ϵ is small, the gain numbers may still be quite large for all practical purposes.

6 Summary

In this first part of our contribution we studied the precision of the baseline before and after ambiguity fixing. This was done for the time-averaged model and for the geometry-based model, where we discriminated between the phase-only case, the code-only case, and the phase-and-code case. Based on the assumption that the relative receiver-satellite geometry changes smoothly with time, a second-order approximation was given of the baseline variance matrices.

Motivated by the purpose of ambiguity fixing, which is to improve upon the precision of the baseline, we introduced a measure for the gain in baseline precision

and showed how it relates to the change over time of the receiver-satellite geometry. The gain numbers which measure the improvement in baseline precision lie in the interval $[1, \infty)$. They become infinite in case of instantaneous positioning, they are large for short observation time-spans and they get smaller as time progresses. It was shown that the gain numbers follow an inverse square law in the observation time-span and that they can be enlarged by a factor of at most 3, through an increase in the sampling rate.

The gain-number concept also allowed us to formulate canonical forms of the various baseline variance matrices. Since they provide for a simultaneous diagonalization of the variance matrices, they give a direct and transparant way of comparing the properties of the baseline precision; not only when different measurement scenarios are used, but also when using either the geometry-based model or the time-averaged model. They also revealed how the change in the receiver-satellite geometry competes with the phase-code variance ratio.

In *Part II* we will focus our attention on the second set of parameters in the single-baseline model, the carrier phase ambiguities. This is done for the geometry-free model, the time-averaged model, and the geometry-based model. We will study the precision and correlation of both the DD ambiguities and the widelane ambiguities. And as it turns out, it is again the gain numbers which allow us to describe the intrinsic characteristics of the ambiguity precision and correlation.

Appendix

Proof of Theorem 1 (*Floated-baseline precision*)

With the geometry-based single-baseline model of Sect. 2, the linear system of normal equations follows as

$$\begin{bmatrix} N_b & N_{ba} \\ N_{ab} & N_a \end{bmatrix} \begin{bmatrix} \hat{b} \\ \hat{a} \end{bmatrix} = \begin{bmatrix} r_b \\ r_a \end{bmatrix} \ , \tag{31}$$

with

$$N_b = (\alpha_1 + \alpha_2 + \beta_1 + \beta_2) \sum_{i=1}^{k} A_i^T P A_i \ ,$$

$$N_{ba} = k\left[\alpha_1 \lambda_1 \bar{A}^T D^{+T} \ , \ \alpha_2 \lambda_2 \bar{A}^T D^{+T}\right] \ ,$$

$$N_a = k \ \mathrm{diag}(\alpha_1 \lambda_1^2, \alpha_2 \lambda_2^2) \otimes (D^T D)^{-1} \ ,$$

and

$$r_b = \sum_{i=1}^{k} A_i^T P d(i) \ ,$$

$$r_a = k\left[\alpha_1 \bar{\phi}_1^T D^{+T}, \alpha_2 \bar{\phi}_2^T D^{+T}\right]^T \ ,$$

$$d(i) = (\alpha_1 + \alpha_2)\phi_w(i) + (\beta_1 + \beta_2) p_w(i) \ ,$$

with the time and weighted averages

$$\bar{\phi}_1 = \frac{1}{k} \sum_{i=1}^{k} \phi_1(i), \quad \bar{\phi}_2 = \frac{1}{k} \sum_{i=1}^{k} \phi_2(i) \ ,$$

$$\phi_w(i) = \frac{\alpha_1 \phi_1(i) + \alpha_2 \phi_2(i)}{\alpha_1 + \alpha_2}, \quad p_w(i) = \frac{\beta_1 p_1(i) + \beta_2 p_2(i)}{\beta_1 + \beta_2} \ ,$$

and where D^+ is the pseudo-inverse of D. Note that N_b and r_b are independent of the chosen reference satellite. Since the weight matrix of the floated baseline reads as

$$Q_{\hat{b}}(\phi, p)^{-1} = N_b - N_{ba} N_a^{-1} N_{ab} \ ,$$

we obtain after substitution and inversion

$$Q_{\hat{b}}(\phi, p) = \left[(\beta_1 + \beta_2) \left(k \bar{A}^T P \bar{A} + (1 + 1/\epsilon) \sum_{i=1}^{k} (A_i - \bar{A})^T P (A_i - \bar{A}) \right) \right]^{-1} \ , \tag{32}$$

with $\epsilon = (\beta_1 + \beta_2)/(\alpha_1 + \alpha_2)$. The variance matrix $Q_{\hat{b}}(\phi)$ follows then from setting $\beta_1 = 0$ and $\beta_2 = 0$, and the variance matrix $Q_{\hat{b}}(p)$ from setting $\alpha_1 = 0$ and $\alpha_2 = 0$. *End of proof.* □

Proof of Theorem 2 (*Fixed-baseline precision*)

Since the weight matrix of the fixed baseline reads as

$$Q_{\check{b}}(\phi, p)^{-1} = N_b = \left[(\alpha_1 + \alpha_2 + \beta_1 + \beta_2) \sum_{i=1}^{k} A_i^T P A_i \right] \ , \tag{33}$$

it follows by setting $\beta_1 = \beta_2 = 0$ that

$$Q_{\check{b}}(\phi) = \left[(\alpha_1 + \alpha_2) \sum_{i=1}^{k} A_i^T P A_i \right]^{-1} \ .$$

This together with

$$Q_{\hat{b}}(p) = \left[(\beta_1 + \beta_2) \sum_{i=1}^{k} A_i^T P A_i \right]^{-1}$$

of Theorem 1, shows that

$$Q_{\check{b}}(\phi, p) = \left[Q_{\hat{b}}(p)^{-1} + Q_{\check{b}}(\phi)^{-1} \right]^{-1} \ .$$

End of proof. □

Proof of Theorem 3 (*Baseline precision to second order*)

It follows from taking the time average of the second-order approximation

$$a_j(t_i) \doteq a_j(t_c) + \dot{a}_j(t_c)(t_i - t_c) + \tfrac{1}{2} \ddot{a}_j(t_c)(t_i - t_c)^2$$

that

$$\bar{a}_j \doteq a_j(t_c) + \tfrac{1}{2}\ddot{a}_j(t_c)\tfrac{1}{k}\sum_{i=1}^{k}(t_i - t_c)^2 \ .$$

The difference of these two equations gives

$$a_j(t_i) - \bar{a}_j \doteq \dot{a}_j(t_c)p_i + \ddot{a}_j(t_c)q_i$$

or

$$A_i - \bar{A} \doteq \dot{A}p_i + \ddot{A}q_i \ , \tag{34}$$

with

$$p_i = (t_i - t_c) \ \text{ and } \ q_i = \frac{1}{2}\left(p_i^2 - \frac{1}{k}\sum_{i=1}^{k}p_i^2\right) \ . \tag{35}$$

With Eq. (34), we have the approximation

$$\begin{aligned}&(A_i - \bar{A})^T P(A_i - \bar{A}) \doteq \\ &\dot{A}^T P\dot{A}p_i^2 + (\dot{A}^T P\ddot{A} + \ddot{A}^T P\dot{A})p_i q_i + \ddot{A}^T P\ddot{A}q_i^2 \ .\end{aligned} \tag{36}$$

Using the identities

$$\sum_{i=1}^{k} i = \frac{1}{2}k(k+1) \ ,$$

$$\sum_{i=1}^{k} i^2 = \frac{1}{6}k(k+1)(2k+1) \ ,$$

$$\sum_{i=1}^{k} i^3 = \frac{1}{4}k^2(k+1)^2 \ ,$$

$$\sum_{i=1}^{k} i^4 = \frac{1}{30}k(k+1)(2k+1)(3k^2+3k-1) \ ,$$

it follows with $t_i = t_0 + iT$, $t_c = \frac{1}{k}\sum_{i=1}^{k} t_i$ and Eq. (35) that

$$\sum_{i=1}^{k} p_i^2 = \frac{1}{12}kT^2(k^2-1) \ ,$$

$$\sum_{i=1}^{k} p_i q_i = 0 \ ,$$

$$\sum_{i=1}^{k} q_i^2 = \frac{1}{720}kT^4(k^2-1)(k^2-4) \ .$$

Using this result together with Eq. (36), shows that

$$\begin{aligned}&(A_i - \bar{A})^T P(A_i - \bar{A}) \doteq \\ &\frac{1}{12}kT^2(k^2-1)\left[\dot{A}^T P\dot{A} + \frac{1}{60}T^2(k^2-4)\ddot{A}^T P\ddot{A}\right] \ .\end{aligned} \tag{37}$$

The theorem now follows from substituting Eq. (37) into the expression for $Q_{\hat{b}}(\phi, p)$ of Corollary 1.
End of proof. □

Proof of Theorem 4 (*Range of gain numbers*)

Case (*i*): We will assume that the variance matrices of the baseline are positive definite, both for the float and for the fixed solution. Thus $Q_{\hat{b}}(\phi) > 0$ and $Q_{\check{b}}(\phi) > 0$. The positive gain numbers $\gamma_i > 0$, $i = 1, 2, 3$, therefore satisfy

$$\begin{aligned}0 &= \mid Q_{\hat{b}}(\phi) - \gamma_i Q_{\check{b}}(\phi) \mid \\ &= \mid -\gamma_i Q_{\hat{b}}(\phi) \mid\mid Q_{\check{b}}^{-1}(\phi) - \frac{1}{\gamma_i}Q_{\check{b}}^{-1}(\phi) \mid\mid Q_{\hat{b}}(\phi) \mid \ ,\end{aligned}$$

from which it follows that

$$\frac{1}{\gamma_i} = \frac{b_i^T Q_{\hat{b}}^{-1}(\phi) b_i}{b_i^T Q_{\check{b}}^{-1}(\phi) b_i}$$

for some $b_i \neq 0$. Substitution of

$$Q_{\hat{b}}^{-1}(\phi) = Q_{\check{b}}^{-1}(\phi) - (\alpha_1 + \alpha_2)k\bar{A}^T P\bar{A}$$

gives

$$(1 - 1/\gamma_i) = (\alpha_1 + \alpha_2)k\frac{b_i^T \bar{A}^T P\bar{A} b_i}{b_i^T Q_{\check{b}}^{-1}(\phi) b_i} \ .$$

This shows, since $\bar{A}^T P\bar{A}$ is positive semi definite, that $\gamma_i \geq 1$ and therefore that $\gamma(f) \geq 1$, for all $f \in R^3$.
Case (*ii*): From the above equation, it also follows that $\gamma_i > 1$ and therefore that $\gamma(f) > 1$, for all $f \in R^3$, if and only if $N(\bar{A}^T P\bar{A}) = \{\emptyset\}$. Hence, γ_i reaches its smallest possible value of 1 if and only if $b_i \in N(\bar{A}^T P\bar{A})$, which shows that the number of gain numbers that equal one is given by the dimension of the nullspace $N(\bar{A}^T P\bar{A})$.
Case (*iii*): When $A_i = \bar{A}$ for $i = 1, \ldots, k$, $Q_{\hat{b}}(\phi)^{-1} = (\alpha_1 + \alpha_2)k\bar{A}^T P\bar{A}$, showing with the above equation that $\gamma_i = \infty$, $i = 1, 2, 3$. The reverse follows likewise, since the vectors b_i are eigenvectors and thus linear independent.
End of proof. □

Proof of Theorem 5 (*Gain numbers and principal angles*)

The principal angles $\theta_i \in [0, \pi/2]$ between the subspaces $R(U)$ and $R(V)$ are defined recursively as

$$\cos\theta_i = \max_{u \in R(U)} \max_{v \in R(V)} \frac{u^T v}{\sqrt{u^T u v^T v}} = \frac{u_i^T v_i}{\sqrt{u_i^T u_i v_i^T v_i}} \ ,$$

subject to

$$\begin{cases} u^T u_j = 0 & j = 1, \ldots, (i-1) \\ v^T v_j = 0 & j = 1, \ldots, (i-1) \ . \end{cases}$$

From the defining equations for U and V it follows that

$$(\alpha_1 + \alpha_2)U^T U = Q_{\hat{b}}^{-1}(\phi) \ ,$$

$$(\alpha_1 + \alpha_2)U^T V = Q_{\hat{b}}^{-1}(\phi) \ ,$$

$$(\alpha_1 + \alpha_2)V^T V = Q_{\check{b}}^{-1}(\phi) \ .$$

Hence, if we define

$$u = \sqrt{(\alpha_1+\alpha_2)}UQ_{\hat{b}}(\phi)^{1/2}a \ ,$$
$$v = \sqrt{(\alpha_1+\alpha_2)}VQ_{\check{b}}(\phi)^{1/2}b \ ,$$

then

$$u^Tu = a^Ta \ ,$$
$$u^Tv = a^T(Q_{\hat{b}}(\phi)^{-1}Q_{\check{b}}(\phi))^{1/2}b \ ,$$
$$v^Tv = b^Tb \ ,$$

and therefore

$$\frac{u^Tv}{\sqrt{u^Tuv^Tv}} = \frac{a^T(Q_{\hat{b}}(\phi)^{-1}Q_{\check{b}}(\phi))^{1/2}b}{\sqrt{a^Ta}\sqrt{b^Tb}} \ .$$

This shows that the principal angles between $R(U)$ and $R(V)$ follow from solving

$$\cos\theta_i = \max_a \max_b \frac{a^T(Q_{\hat{b}}(\phi)^{-1}Q_{\check{b}}(\phi))^{1/2}b}{\sqrt{a^Ta}\sqrt{b^Tb}}$$

$$= \frac{a_i^T(Q_{\hat{b}}(\phi)^{-1}Q_{\check{b}}(\phi))^{1/2}b_i}{\sqrt{a_i^Ta_i}\sqrt{b_i^Tb_i}} \ ,$$

subject to

$$\begin{cases} a^Ta_j = 0 & j = 1,\ldots,(i-1) \ , \\ b^Tb_j = 0 & j = 1,\ldots,(i-1) \ . \end{cases}$$

Since $\gamma_1 \le \gamma_2 \le \gamma_3$ are the three eigenvalues of $Q_{\hat{b}}(\phi)Q_{\check{b}}(\phi)^{-1}$, their square roots are the singular values of $Q_{\hat{b}}(\phi)^{1/2}Q_{\check{b}}(\phi)^{-1/2}$, from which it follows that $\cos(\theta_i) = 1/\sqrt{\gamma_i}$.
End of proof. □

Proof of Theorem 6 (*Gain, sampling rate, and time-span*)

From the definition of the gain numbers, it follows that

$$\left|Q_{\check{b}}(\phi)^{-1} - \gamma_iQ_{\hat{b}}(\phi)^{-1}\right| = 0 \ .$$

Substitution of

$$Q_{\check{b}}(\phi)^{-1} = (\alpha_1+\alpha_2)\sum_{i=1}^{k}A_i^TPA_i \ ,$$

$$Q_{\hat{b}}(\phi)^{-1} = (\alpha_1+\alpha_2)\sum_{i=1}^{k}(A_i-\bar{A})^TP(A_i-\bar{A}) \ ,$$

gives

$$\left|k\bar{A}^TP\bar{A} - (\gamma_i-1)\sum_{i=1}^{k}(A_i-\bar{A})^TP(A_i-\bar{A})\right| = 0 \ .$$

Substitution of the first-order approximation

$$\sum_{i=1}^{k}(A_i-\bar{A})^TP(A_i-\bar{A}) = \frac{1}{12}kT^2(k^2-1)\dot{A}^TP\dot{A}$$

which follows from Eq. (37), finally gives

$$\left|\bar{A}^TP\bar{A} - \mu_i\dot{A}^TP\dot{A}\right| = 0 \ ,$$

with

$$\gamma_i - 1 = \frac{12\mu_i}{T^2(k^2-1)} \ .$$

End of proof. □

Proof of Theorem 7 (*Canonical decomposition*)

Of the eight cases we only prove the three phase-only cases (*iii*), (*iv*), and (*v*). With the help of Theorems 1 and 2, and the Corollaries 1 and 2, the proofs of the other cases go along similar lines.
Case (*iii*): The gain numbers and gain vectors are related in matrix form as

$$Q_{\hat{b}}(\phi)F = Q_{\check{b}}(\phi)F\Gamma \ . \tag{38}$$

Premultiplication with F^T gives

$$F^TQ_{\hat{b}}(\phi)F = F^TQ_{\check{b}}(\phi)F\Gamma \ . \tag{39}$$

In order to prove (*iii*), it suffices to show that F can be chosen such that $F^TQ_{\check{b}}(\phi)F = I$. It will be clear that the columns of F can always be normalized such that the diagonal terms of $F^TQ_{\check{b}}(\phi)F$ equal one. It therefore remains to be shown that the columns of F are $Q_{\check{b}}(\phi)$-orthogonal. It follows from the definition of the gain numbers that

$$f_i^TQ_{\hat{b}}(\phi)f_j = \begin{cases} \gamma_if_i^TQ_{\check{b}}(\phi)f_j \\ \gamma_jf_i^TQ_{\check{b}}(\phi)f_j \ . \end{cases}$$

This shows that $f_i^TQ_{\check{b}}(\phi)f_j = 0$ if $\gamma_i \neq \gamma_j$. Thus in this case the vectors f_i and f_j are $Q_{\check{b}}(\phi)$-orthogonal. In case $\gamma_i = \gamma_j$, any linear combination of f_i and f_j is again a gain vector that corresponds with $\gamma_i = \gamma_j$. It is therefore always possible to find a linear combination of f_i and f_j that is $Q_{\check{b}}(\phi)$-orthogonal to either f_i or f_j. Hence, also for the case where gain numbers are identical, corresponding gain vectors can be found that are $Q_{\check{b}}(\phi)$-orthogonal. This shows that F can be chosen such that $F^TQ_{\check{b}}(\phi)F = I$ or $Q_{\check{b}}(\phi) = (FF^T)^{-1}$ holds.
Case (*iv*): This result simply follows from $F^TQ_{\check{b}}(\phi)F = I_3$ and Eq. (39).
Case (*v*): Since $Q_{\check{b}}(\bar{\phi}) = [(\alpha_1+\alpha_2)k\bar{A}^TP\bar{A}]^{-1}$, this matrix exists only when $N(\bar{A}^TP\bar{A}) = \{\emptyset\}$. From Corollary 2 follows that

$$Q_{\check{b}}(\bar{\phi}) = \left[Q_{\check{b}}^{-1}(\phi) - Q_{\hat{b}}^{-1}(\phi)\right]^{-1} \ .$$

Substitution of (*iii*) and (*iv*) of Theorem 7 into this expression, proves (*v*).
End of proof. □

References

Borre K (1995) GPS i landmaelingen, Aalborg

Dedes G, Goad CC (1994) Real-Time cm-level GPS Positioning of Cutting Blade and Earth Moving Equipment. Proc 1994 National Technical Meeting ION, San Diego, Calif, pp 587–594

Euler HJ, Goad CC (1990) On Optimal Filtering of GPS Dual Frequency Observations without the using Orbit Information. Bull Geod 65: 130–143

Euler HJ, Hatch R (1994) Comparison of Several AROF Kinematic Techniques. Proc ION-94 San Diego, Calif, pp 363–370

Frei E, Beutler G (1990) Rapid Static Positioning Based on the Fast Ambiguity Resolution Approach FARA: Theory and First Results. Manuscr Geod 15: 325–356

Goad CC (1996) Short Distance GPS Models. In: Kleusberg A, and Teunissen PJG (eds), GPS for Geodesy, Springer, Berlin Heidelberg New York, pp 239–262

Golub GH, van Loan CF (1989) Matrix Computations, 2nd edn. The John Hopkins University Press, Baltimore, Md

Hatch R (1982) The Synergism of GPS Code and Carrier Measurements. Proc 3rd Int Geod Symp Satellite Positioning, Las Cruces, New Mexico, 8–12 February, Vol 2, pp 1213–1231

Hofmann-Wellenhof B, Lichtenegger H, Collins J (1994) Global Positioning System: Theory and Practice, 3rd edn. Springer, Berlin Heidelberg New York

Kleusberg A, Teunissen PJG (eds.) (1996) GPS for Geodesy. Lectures Notes in Earth Sciences, Vol 60, Springer, Berlin Heidelberg New York

Leick A (1995) GPS Satellite Surveying, 2nd edn. John Wiley, New York

Parkinson B , Spilker JJ (eds) (1996) GPS: Theory and Applications, vols 1 and 2. AIAA, Washington, DC

Remondi BW (1985) Performing Centimeter-Level Surveys in Seconds with GPS Carrier Phase: Initial Results. NOAA Technical Memorandum NOS NGS-43, Rockville, MD.

Seeber G (1993) Satellite Geodesy. Walter de Gruyter, Berlin New York

Teunissen PJG (1993) Least-squares estimation of the integer GPS ambiguities. Invited Lecture, Section IV Theory and Methodology, IAG General Meeting, Beijing, China, August. Also in: Delft Geodetic Computing Centre LGR Series 6: p 16

Teunissen PJG (1996) An analytical study of ambiguity decorrelation using dual frequency code and carrier phase. J Geod 70: 515–528

Tiberius CCJM, de Jonge PJ (1995) Fast positioning using the LAMBDA-method. Proc DSNS'95, Bergen, Norway, April 24–28, Paper 30, p 8

Wübbena G (1991) Zur Modellierung von GPS Beobachtungen für die hochgenaue Positions-bestimmung, PhD Thesis, Hannover